Heteronanostructures

DOI: 10.1002/anie.201202128

One-Pot Controlled Synthesis of Hexagonal-Prismatic $Cu_{1.94}S$-ZnS, $Cu_{1.94}S$-ZnS-$Cu_{1.94}S$, and $Cu_{1.94}S$-ZnS-$Cu_{1.94}S$-ZnS-$Cu_{1.94}S$ Heteronanostructures**

*Shi-Kui Han, Ming Gong, Hong-Bin Yao, Ze-Ming Wang, and Shu-Hong Yu**

Colloidal nanocrystals, which have been referred to as "artificial atoms", have been intensively developed during the past decades. These nanocrystals have been grown from many different materials and cheaply produced in fairly large amounts with uniform size and shape.[1] As one particular interesting emerging class of colloidal nanostructures, heterostructured nanocrystals containing two or more chemically distinct components,[2] that is, semiconductor–semiconductor or semiconductor–metal, in one single nanostructure with multifunctional or new properties induced by the heterointerfaces will undoubtedly lead to revolutionary new applications of nanomaterials in various fields, such as photovoltaic devices, high-performance catalysis, biological and biomedical sensing, and a new generation of optoelectronic devices. In particular, enormous efforts have been devoted to preparing heterostructured nanocrystals, including Au-Fe_3O_4,[3] FePt-In_2O_3,[4] Au-Pt-Fe_3O_4,[5] Ag-Ag_2S,[6] CdS-Ag_2S,[7,8] ZnS-Ag_2S,[9,10] Cu_2S-In_2S_3,[11] Cu_2S-$CuInS_2$,[12] Cu_2S-CdS,[13–16] and Bi_2Te_3-Te,[17] which combine optical and/or electrical, magnetic, and catalytic properties.

Copper sulfides ($Cu_{2-x}S$) are excellent p-type semiconductor materials owing to the copper vacancies in the lattice and have gained much attention since the discovery of CdS/Cu_2S heterojunction solar cells in 1954.[18] $Cu_{2-x}S$ compounds possess an x-dependent bandgap energy varying from about 1.2 eV for chalcocite ($x=0$) to 2.0 eV for covellite ($x=1$; $E_g=$ 1.2 eV for Cu_2S, 1.5 eV for $Cu_{1.8}S$, and 2.0 eV for CuS). These values match well with the solar spectrum and the materials are regarded to be effective light-absorbing materials for photovoltaic solar cells.[11] Recently, nanocrystal-based heterojunction solar cells have been prepared by creating thin films that consist of separate layers of p-type and n-type semiconductor nanocrystals[19–22] with the hope of significantly enhancing the performance and reducing the manufacturing cost of solar cells. Owing to the layer of organic surfactant capping agent on the solution-processed nanocrystals, insufficient contact between the two semiconductor components has become a challenge for the design of nanodevices.[15]

Herein, we present a facile one-pot colloidal route for the controlled synthesis of unique hexagonal-prismatic $Cu_{1.94}S$-ZnS, $Cu_{1.94}S$-ZnS-$Cu_{1.94}S$, and $Cu_{1.94}S$-ZnS-$Cu_{1.94}S$-ZnS-$Cu_{1.94}S$ heteronanostructures with screw-, dumbbell-, and sandwich-like shapes by using CuI and $[Zn(S_2CNEt_2)_2]$ as precursors in oleylamine.

Figure 1a shows the X-ray diffraction (XRD) pattern of the colloidal heteronanostructures prepared by using CuI and $[Zn(S_2CNEt_2)_2]$ with a molar ratio of 13:6.5. Based on the XRD pattern, we can see that the prepared colloidal heteronanostructures are composed of crystalline phases of $Cu_{1.94}S$ (JCPDS No. 23-0959; monoclinic, $a=26.897$, $b=15.745$, $c=13.565$ Å) and wurtzite ZnS (JCPDS No. 36-1450). A typical transmission electron microscopy (TEM) image (Figure 1b) reveals that each particle is a hexagonal prism with a length of about 60 nm and a diameter of 30 nm.

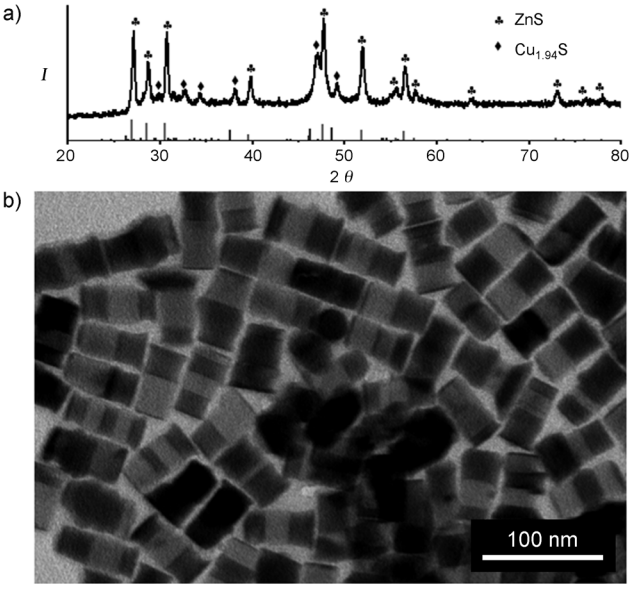

Figure 1. a) XRD pattern and b) TEM image of the as-prepared heteronanostrutures with a screw-like shape.

[*] Dr. S. K. Han, M. Gong, H. B. Yao, Z. M. Wang, Prof. Dr. S. H. Yu
Division of Nanomaterials and Chemistry, Hefei National Laboratory for Physical Sciences at Microscale, Department of Chemistry, National Synchrotron Radiation Laboratory, University of Science and Technology of China
Hefei, Anhui 230026 (P.R. China)
E-mail: shyu@ustc.edu.cn
Homepage: http://staff.ustc.edu.cn/~yulab/

[**] This work is supported by the National Basic Research Program of China (2010CB934700), the National Natural Science Foundation of China (Nos. 91022032, 21061160492, J1030412), Chinese Academy of Sciences (Grant KJZD-EW-M01-1), International Science & Technology Cooperation Program of China (Grant 2010DFA41170), and the Principal Investigator Award by the National Synchrotron Radiation Laboratory at the University of Science and Technology of China.

Supporting information for this article is available on the WWW under http://dx.doi.org/10.1002/anie.201202128.

Furthermore, high-resolution TEM (HRTEM) confirms the orientational relationship between $Cu_{1.94}S$ and ZnS nanostructures (Figure 2a). The analysis of the lattice spacing reveals that the (100) planes ($d = 26.9$ Å) of $Cu_{1.94}S$ are coincident with the (002) planes ($d = 3.1$ Å) of ZnS, which fits the structure model for such a heterostructure well (Figure 2b).

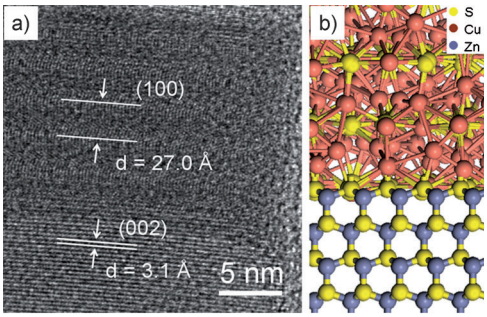

Figure 2. a) A typical HRTEM image of the as-prepared heteronanostructures. b) Model of the atomic arrangements of the epitaxial planes for (100) $Cu_{1.94}S$ and (002) ZnS.

A high-angle annular dark field scanning TEM (HAADF-STEM) image of the heteronanostructures (Figure 3) reveals a clear contrast between the two side parts and the middle part and hints that the heteronanostructure is indeed composed of two different materials similar to that of "dumbbell" structures. As shown in Figure 3, the STEM-EDS elemental mapping was applied to obtain elemental distributions of Cu and Zn in the two-component heteronanostructures. The green regions in the image shown in Figure 3 are the Cu-containing portions of the nanostructures, whereas the red regions are the Zn-containing segments, demonstrating that the segments on the both sides of the nanostructures are $Cu_{1.94}S$, while the middle part is ZnS.

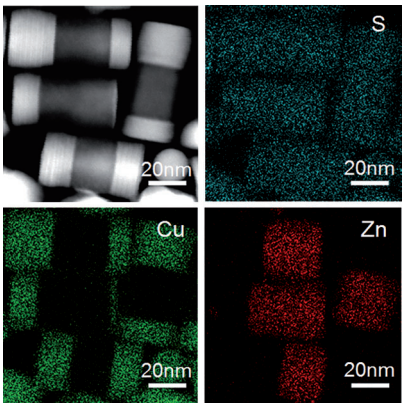

Figure 3. STEM-EDS elemental mapping images of the as-prepared $Cu_{1.94}S$-ZnS-$Cu_{1.94}S$ heteronanostructures with a dumbbell-like shape.

Increasing the Zn^{2+} source of $[Zn(S_2CNEt_2)_2]$ results in morphological changes similar to that of sandwich structures. The segments of the $Cu_{1.94}S$ become thinner in length and larger in diameter compared with the "dumbbell" structures shown in Figure 4, whereas a new segment of $Cu_{1.94}S$ appears in the middle and separates the ZnS into two parts. It is also revealed by XRD patterns (Supporting Information, Figure S1). Because of the ratio of CuI/$[Zn(S_2CNEt_2)_2]$ decreased, the diffraction peaks belonging to $Cu_{1.94}S$ phase become weaker, and peaks belonging to ZnS phase became stronger in intensity.

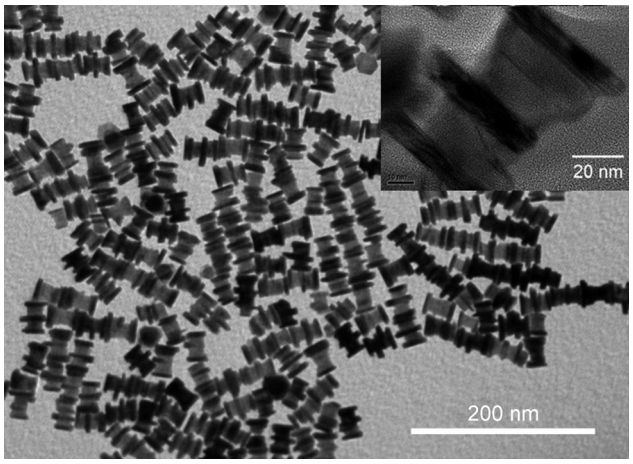

Figure 4. A typical TEM image of complex $Cu_{1.94}S$-ZnS-$Cu_{1.94}S$-ZnS-$Cu_{1.94}S$ sandwich-like heteronanostructures prepared by using CuI and $[Zn(S_2CNEt_2)_2]$ as precursors with a molar ratio of 13:8. Inset: a high-resolution TEM image of a typical example of such a heteronanostructure.

To the best of our knowledge, two-component nanostructures with hexagonal-prismatic morphology can be rarely prepared by a facile one-pot colloidal synthetic approach. Up to now, the synthesis of semiconductor heterostructures through wet chemistry is known to proceed predominantly by either seeded or catalyst-assisted growth modes.[9] To understand the formation mechanism for the present $Cu_{1.94}S$-ZnS heterostructured systems, a series of experiments were performed. First of all, we observed that when CuI and $[Zn(S_2CNEt_2)_2]$ were mixed together in oleylamine, the solution turned brown immediately, indicating that Cu^+ reacted with $[Zn(S_2CNEt_2)_2]$ forming $[Cu(S_2CNEt_2)]$, as only $[Zn(S_2CNEt_2)_2]$ in oleylamine is colorless and CuI is green. We studied the evolution of the "sandwich" heterostructures by taking aliquots over the course of the reaction (Supporting Information, Figure S2). The $[Cu(S_2CNEt_2)]$ decomposed to form $Cu_{1.94}S$ egg-shape nanocrystals at first when the temperature reached 150 °C. As the reaction proceeded, the egg-shaped nanocrystals grew up from about 20 nm to 50 nm in length. The shape changed very quickly from egg-shaped to sandwich-like heterostructures in 30 s with the color of the solution changing into grayish-green from brown. Compared with the hexagonal-phase Cu_2S, monoclinic $Cu_{1.94}S$ has high cationic mobility and therefore has more cationic vacancies, which is of benefit for a foreign anion dissolving.[10] We presumed that the evolution of the heterostructures involved Zn^{2+} cations exchanging in egg-shape $Cu_{1.94}S$ nanocrystals and then a restructuring of the ZnS and $Cu_{1.94}S$, which was very sensitive to the concentration of the solution. To provide direct evidence, we reduced the dose

of the CuI and $[Zn(S_2CNEt_2)_2]$ to one-fifth of their original. Zn^{2+} exchanged in egg-shape $Cu_{1.94}S$ nanocrystals (Supporting Information, Figure S3), but restructuring process did not occur. It is obvious that the restructuring process does not occur at low concentrations.

To gain more understanding of the formation mechanism, we performed a series of experiments by varying the molar ratio of CuI/$[Zn(S_2CNEt_2)_2]$. When the molar ratio of CuI/$[Zn(S_2CNEt_2)_2]$ was increased to 13:5.5, we mainly observed "screw"-shaped heterostructures (Supporting Information, Figure S4b). To further increase the molar ratio to 13:4, we could not obtain $Cu_{1.94}S$-ZnS heterostructures but a mixture of $Cu_{1.94}S$ and ZnS egg-shaped nanocrystals (Supporting Information, Figure S4a). In contrast, upon decreasing the molar ratio to 13:14, the hexagonal prism-like heterostructures disappeared (Supporting Information, Figure S4f), but irregular structures formed instead. On the basis of the results stated above, it can be concluded that the formation process of the hexagonal-prismatic $Cu_{1.94}S$-ZnS heterostructures (Scheme 1). First, $[Cu(S_2CNEt_2)]$ precursor will form by reacting of Cu^+ and $[Zn(S_2CNEt_2)_2]$. Then, $[Cu(S_2CNEt_2)]$ decomposed to form $Cu_{1.94}S$ egg-shape nanocrystals as seeds at first when the temperature reached 150 °C. When the molar ratio of CuI/$[Zn(S_2CNEt_2)_2]$ is 13:4, there is also many dissociative Cu^+ ions in the solution that are still more than Zn^{2+} (the molar ratio of Cu^+/Zn^{2+} being 5:4). Under this condition, only a mixture of $Cu_{1.94}S$ and ZnS nanocrystals was obtained. While decreasing the ratio to 13:5.5, the dissociative Cu^+ is also existence in solution (the molar ratio of Cu^+/Zn^{2+} being 2:5.5). As the reaction processed, cation exchange occurred at one tip of the egg-shape $Cu_{1.94}S$ nanocrystals and the energetic interfaces as reaction fronts proceed through the nanocrystals. At the same time, the dissociative Cu^+ and Zn^{2+} ions react with a large amount S^{2-} to grow along the 100 direction of $Cu_{1.94}S$ and 002 direction of ZnS simultaneously and separately to form screw-like $Cu_{1.94}S$-ZnS heterostructures. Adjusting the molar ratio to 13:6.5, the reaction between Cu^+ and $[Zn(S_2CNEt_2)_2]$ is complete and only $[Cu(S_2CNEt_2)]$ and Zn^{2+} exist in the reaction solution. Because of the increase of the Zn source to 0.065 mmol, the ZnS grows further inward from either end, and more Cu^+ is released, which will combine with the dissociative S^{2-} for growing and restructuring on the other end of the ZnS to form the dumbbell-like $Cu_{1.94}S$-ZnS-$Cu_{1.94}S$ heterostructures. As decreasing the molar ratio to 13:8, a portion of $[Zn(S_2CNEt_2)_2]$ is also in solution. After the formation of the egg-shape $Cu_{1.94}S$ nanocrystals, the cation-exchange reaction occurs at both ends of the egg-shape $Cu_{1.94}S$ nanocrystals, and the restructuring and Ostwald ripening process follows soon afterwards to form the sandwich-like $Cu_{1.94}S$-ZnS-$Cu_{1.94}S$-ZnS-$Cu_{1.94}S$ heterostructures. Finally, decreasing the ratio to 13:14, the hexagonal prism heterostructures disappeared and the irregular structures formed instead.

The optical absorption spectra of the different $Cu_{1.94}S$-ZnS nanostructures show significant absorbance across the solar spectrum and a broad near-infrared (NIR) absorption between 800 nm and 2000 nm (Supporting Information, Figure S5). The broad NIR absorption observed in the spectra is derived from a surface plasmon resonance for copper sulfide with a relatively high carrier (holes) concentration exhibiting strong free carrier absorption.[23,24] The absorption peak located at 332 nm (3.7 eV) with a slight blue shift compared with the bulk wurtzite ZnS (3.8 eV)[25] is attributed to the quantum confine effects and the coupling between $Cu_{1.94}S$ and ZnS.[9] Owing to their significant absorbance across the solar spectrum and broad NIR absorption, the utility of these nanoscale heterostructures as the active component in heterojunction solar cells or optical sensors will be evaluated in future work.

In summary, unique hexagonal-prismatic $Cu_{1.94}S$-ZnS, $Cu_{1.94}S$-ZnS-$Cu_{1.94}S$, and $Cu_{1.94}S$-ZnS-$Cu_{1.94}S$-ZnS-$Cu_{1.94}S$ heteronanostructures with screw-, dumbbell-, and sandwich-like shapes can be synthesized by controlling the molar ratio of CuI and $[Zn(S_2CNEt_2)_2]$ in oleylamine. This colloid method may provide a new way for controlled growth of a family of metal chalcogenide heteronanostructures with interesting optical properties or multifunctionality for applications in optoelectronic devices, such as solar cells and optical sensing.

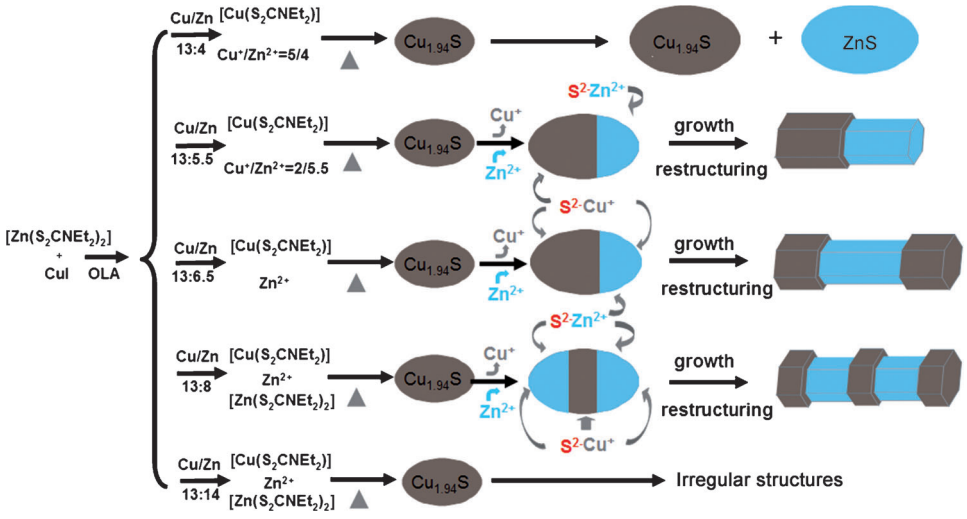

Scheme 1. Synthetic routes for preparation of different hexagonal prism $Cu_{1.94}S$-ZnS heteronanostructures.

Experimental Section

Sodium *N*,*N*-diethyldithiocarbamate ($Na(S_2CNEt_2)$), $ZnSO_4{\cdot}7H_2O$, and CuI were purchased from Shanghai Reagent Company (P.R. China). Oleylamine (OLA, 70%) was purchased from Aldrich.

Synthesis of $[Zn(S_2CNEt_2)_2]$ precursors: $Na(S_2CNEt_2)$ (3 g) and $ZnSO_4{\cdot}7H_2O$ (3 g) were first dissolved in distilled water (100 mL and 50 mL, respectively). Then, the two solutions were mixed with stirring in a 500 mL beaker for 1 h. And the resulting white precipitate was filtered, washed several times with distilled water, and dried under a vacuum at 60 °C.

Synthesis of dumbbell-like $Cu_{1.94}S$-ZnS heterostructures: In a typical procedure, CuI (0.13 mmol), $[Zn(S_2CNEt_2)_2]9$ (0.065 mmol), and 5 mL OLA were added in a 25 mL three-necked flask. The mixture was degassed under vacuum at ambient conditions for 20 min. The solution was heated under nitrogen to 150 °C at a rate of 10 °C min^{-1}, and kept at 150 °C for 30 min and then cooled to room temperature. The black product was collected by centrifugation (8000 rpm, 5 min) and washed several times with n-hexane and absolute ethanol for further characterization. By changing the molar ratio of $[Zn(S_2CNEt_2)_2]$ to the other reagents, other heteronanostructures could be obtained.

Received: March 17, 2012
Published online: May 29, 2012

Keywords: cation exchange · copper sulfides · heteronanostructures · semiconductors · zinc sulfides

[1] Y. D. Yin, A. P. Alivisatos, *Nature* **2005**, *437*, 664 – 670.
[2] C. M. Donegá, *Chem. Soc. Rev.* **2011**, *40*, 1512 – 1546.
[3] J. S. Beveridge, M. R. Buck, J. F. Bondi, R. Misra, P. Schiffer, R. E. Schaak, M. E. Williams, *Angew. Chem.* **2011**, *123*, 10049 – 10053; *Angew. Chem. Int. Ed.* **2011**, *50*, 9875 – 9879.
[4] H. M. Wu, O. Chen, J. Q. Zhuang, J. Lynch, D. LaMontagne, Y. Nagaoka, Y. C. Cao, *J. Am. Chem. Soc.* **2011**, *133*, 14327 – 14337.
[5] M. R. Buck, J. F. Bondi, R. E. Schaak, *Nat. Chem.* **2011**, *4*, 37 – 44.
[6] M. L. Pang, J. Y. Hu, H. C. Zeng, *J. Am. Chem. Soc.* **2010**, *132*, 10771 – 10785.
[7] B. Sadtler, D. O. Demchenko, C. K. Erdonmez, L. W. Wang, A. P. Alivisatos, *Science* **2007**, *317*, 355 – 358.
[8] D. O. Demchenko, R. D. Robinson, B. Sadtler, C. K. Erdonmez, A. P. Alivisatos, L. W. Wang, *ACS Nano* **2008**, *2*, 627 – 636.
[9] S. L. Shen, Y. J. Zhang, L. Peng, Y. P. Du, Q. B. Wang, *Angew. Chem.* **2011**, *123*, 7253 – 7256; *Angew. Chem. Int. Ed.* **2011**, *50*, 7115 – 7118.
[10] G. X. Zhu, Z. Xu, *J. Am. Chem. Soc.* **2011**, *133*, 148 – 157.
[11] W. Han, L. X. Yi, N. Zhao, A. W. Tang, M. Y. Gao, Z. Y. Tang, *J. Am. Chem. Soc.* **2008**, *130*, 13152 – 13161.
[12] S. T. Connor, C. M. Hsu, B. D. Weil, S. Aloni, Y. Cui, *J. Am. Chem. Soc.* **2009**, *131*, 4962 – 4966.
[13] B. Sadtler, D. O. Demchenko, H. M. Zheng, S. M. Hughes, M. G. Merkle, U. Dahmen, L. W. Wang, A. P. Alivisatos, *J. Am. Chem. Soc.* **2009**, *131*, 5285 – 5293.
[14] J. B. Rivest, S. L. Swisher, L. K. Fong, H. M. Zheng, A. P. Alivisatos, *ACS Nano* **2011**, *5*, 3811 – 3816.
[15] M. D. Regulacio, C. Ye, S. H. Lim, M. Bosman, L. Polavarapu, W. L. Koh, J. Zhang, Q. H. Xu, M. Y. Han, *J. Am. Chem. Soc.* **2011**, *133*, 2052 – 2055.
[16] J. Y. Tang, Z. Y. Huo, S. Brittman, H. W. Gao, P. D. Yang, *Nat. Nanotechnol.* **2011**, *6*, 568 – 572.
[17] W. S. Wang, J. Goebl, L. H, S. Aloni, Y. X. Hu, L. Zhen, Y. D. Yin, *J. Am. Chem. Soc.* **2010**, *132*, 17316 – 17324.
[18] Y. X. Zhao, H. C. Pan, Y. B. Lou, X. F. Qiu, J. J. Zhu, C. Burda, *J. Am. Chem. Soc.* **2009**, *131*, 4253 – 4261.
[19] I. Gur, N. A. Fromer, M. L. Geier, A. P. Alivisatos, *Science* **2005**, *310*, 462 – 465.
[20] Y. Wu, C. Wadia, W. L. Ma, B. Sadtler, A. P. Alivisatos, *Nano Lett.* **2008**, *8*, 2551 – 2555.
[21] J. Tang, K. W. Kemp, S. Hoogland, K. S. Jeong, H. Liu, L. Levina, M. Furukawa, X. H. Wang, R. Debnath, D. Cha, K. W. Chou, A. Fischer, A. Amassian, J. B. Asbury, E. H. Sargent, *Nat. Mater.* **2011**, *10*, 765 – 771.
[22] X. H. Wang, G. I. Koleilat, J. Tang, H. Liu, I. J. Kramer, R. Debnath, L. Brzozowski, D. A. R. Barkhouse, L. Levina, S. Hoogland, E. H. Sargent, *Nat. Photonics* **2011**, *5*, 480 – 484.
[23] S. W. Hsu, K. On, A. R. Tao, *J. Am. Chem. Soc.* **2011**, *133*, 19072 – 19075.
[24] C. M. Hessel, V. P. Pattani, M. Rasch, M. G. Panthani, B. Koo, J. W. Tunnell, B. A. Korgel, *Nano Lett.* **2011**, *11*, 2560 – 2566.
[25] S. H. Yu, M. Yoshimura, *Adv. Mater.* **2002**, *14*, 296 – 300.

